Quantitative changes in the elasticity and adhesive properties of Escherichia coli ZK1056 prey cells during predation by Bdellovibrio bacteriovorus 109J

ARTICLE *in* LANGMUIR · JULY 2008

Impact Factor: 4.46 · DOI: 10.1021/la8009354 · Source: PubMed

5 AUTHORS, INCLUDING:

Catherine Volle
Cottey College
11 PUBLICATIONS **142** CITATIONS
SEE PROFILE

Katherine Aidala
Mount Holyoke College
44 PUBLICATIONS **297** CITATIONS
SEE PROFILE

Eileen M Spain
Occidental College
48 PUBLICATIONS **1,108** CITATIONS
SEE PROFILE

Megan E Núñez
Mount Holyoke College
36 PUBLICATIONS **1,116** CITATIONS
SEE PROFILE

Quantitative Changes in the Elasticity and Adhesive Properties of *Escherichia coli* ZK1056 Prey Cells During Predation by *Bdellovibrio bacteriovorus* 109J

Catherine B. Volle,[†,⊥] Megan A. Ferguson,[§,⊥] Katherine E. Aidala,[‡] Eileen M. Spain,[||] and Megan E. Núñez*[,†]

Departments of Chemistry and Physics, Mount Holyoke College, South Hadley, Massachusetts 01075, Department of Chemistry, State University of New York, New Paltz, New York 12561, and Department of Chemistry, Occidental College, Los Angeles, California 90041

Received January 29, 2008. Revised Manuscript Received April 29, 2008

Atomic force microscopy (AFM) was used to explore the changes that occur in *Escherichia coli* ZK1056 prey cells while they are being consumed by the bacterial predator *Bdellovibrio bacteriovorus* 109J. Invaded prey cells, called bdelloplasts, undergo substantial chemical and physical changes that can be directly probed by AFM. In this work, we probe the elasticity and adhesive properties of uninvaded prey cells and bdelloplasts in a completely native state in dilute aqueous buffer without chemical fixation. Under these conditions, the rounded bdelloplasts were shown to be shorter than uninvaded prey cells. More interestingly, the extension portions of force curves taken on both kinds of cells clearly demonstrate that bdelloplasts are softer than uninvaded prey cells, reflecting a decrease in bdelloplast elasticity after invasion by *Bdellovibrio* predators. On average, the spring constant of uninvaded *E. coli* cells (0.23 ± 0.02 N/m) was 3 times stiffer than that of the bdelloplast (0.064 ± 0.001 N/m) when measured in a HEPES−metals buffer. The retraction portions of the force curves indicate that compared to uninvaded *E. coli* cells bdelloplasts adhere to the AFM tip with much larger pull-off forces but over comparable retraction distances. The strength of these adhesion forces decreases with increasing ionic strength, indicating that there is an electrostatic component to the adhesion events.

Introduction

Bdellovibrio bacteriovorus 109J is a small, motile, gram-negative bacterium that is characterized by a two-phase life cycle (Figure 1).[1–4] In the "attack phase" of its life cycle, *Bdellovibrio* uses its polar flagellum to swim rapidly but randomly through its environment, hunting for gram-negative prey. When the *Bdellovibrio* predator collides with a prey cell, it first attaches weakly and transiently and then more strongly to the prey cell surface.[5] Using a combination of chemical and mechanical tools, the predator breaches the prey's outer membrane and burrows into the periplasm of the prey (the domain between the outer and inner membranes).[6,7] There the predator stops the prey's respiration and begins to digest and absorb the prey cell. The dead, invaded prey cell with the growing *Bdellovibrio* living inside of it is termed a bdelloplast. As the *Bdellovibrio* takes up amino acids, nucleotides, and lipids along with other biomaterials from the prey cell, it elongates inside the bdelloplast.[4] When the prey has been entirely consumed, the *Bdellovibrio* divides into progeny cells that develop their own flagella and burst out of the prey cell, leaving bits of the cellular membranes and other debris behind.[8] The entire process takes roughly 3 to 4 h, depending on the prey and environment. The stages of the life cycle and the basic architecture of the *Bdellovibrio* and bdelloplast such as the size, shape, and presence of a flagellum were revealed by light and electron microscopy.[7,9–12]

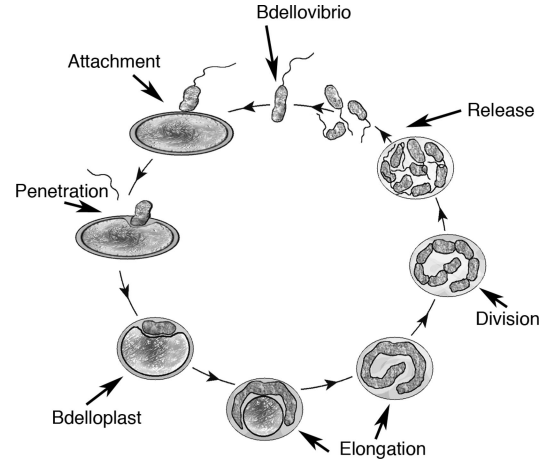

Figure 1. Schematic of the growth cycle of *Bdellovibrio bacteriovorus* 109J. The intraperiplasmic growth cycle is characterized by penetration into the prey cell by the *Bdellovibrio* (top left), rounding of the prey cell into the bdelloplast (bottom left), growth in the prey periplasm (bottom right), and finally release of the progeny cells to start the cycle again (top right).

* To whom correspondence should be addressed. E-mail: menunez@mtholyoke.edu. Phone: (413) 538-2449. Fax (413) 538-2327.
† Department of Chemistry, Mount Holyoke College.
‡ Department of Physics, Mount Holyoke College.
§ State University of New York.
|| Occidental College.
⊥ Both authors contributed equally to this work.

(1) Ruby, E. G. In *The Prokaryotes: A Handbook on the Biology of Bacteria: Ecophysiology, Isolation, Identification, Applications*, 2nd ed.; Balows, A., Truper, H. G., Dworkin, M., Harder, W., Schleifer, K.-H., Eds.; Springer-Verlag: New York, 1991; Vol. *IV*, pp 3400−3415.
(2) Martin, M. O. *J. Mol. Microbiol. Biotechnol.* **2002**, *4*, 5–16.
(3) Rittenberg, S. C. *ASM News* **1983**, *49*, 435–439.
(4) Diedrich, D. L. *Microbiol. Sci.* **1988**, *5*, 100–103.
(5) Seidler, R. J.; Starr, M. P. *J. Bacteriol.* **1969**, *97*, 912–923.
(6) Rittenberg, S. C.; Shilo, M. *J. Bacteriol.* **1970**, *102*, 149–160.
(7) Abram, D.; e Melo, J. C.; Chou, D. *J. Bacteriol.* **1974**, *118*, 663–680.
(8) Kessel, M.; Shilo, M. *J. Bacteriol.* **1976**, *128*, 477–480.
(9) Abram, D.; Davis, B. K. *J. Bacteriol.* **1970**, *104*, 948–965.
(10) Seidler, R. J.; Starr, M. P. *J. Bacteriol.* **1968**, *95*, 1952–1955.
(11) Snellen, J. E.; Starr, M. P. *Arch. Microbiol.* **1974**, *100*, 179–195.
(12) Starr, M. P.; Baigent, N. L. *J. Bacteriol.* **1966**, *91*, 2006–2017.

10.1021/la8009354 CCC: $40.75
Published on Web 06/24/2008

Recently we characterized the interaction of *Bdellovibrio bacteriovorus* 109J with simple biofilms of prey organisms using atomic force microscopy (AFM).[13–15] Biofilms, communities of microorganisms attached to an interface, are notoriously resistant to destruction by chemical or physical means as well as by bacteriophages and antibiotics.[16–20] Biofilms present an interesting research opportunity because this complex form of microbial development is relevant to medicine, agriculture, food processing, and many other fields.[18] In our earlier work, *E. coli* ZK1056 biofilms were grown in dilute growth media at an air−liquid interface on partially submerged coverslips, and bdellovibrios were added to determine whether the predator could destroy biofilms.[14] When grown in full-strength nutrient broth, bdellovibrios were able to consume biofilm cells but were not able to remove the film completely. Under dilute nutrient conditions that better reflect the natural environment, bdellovibrios could both prevent simple biofilms from forming and clear established biofilms. Moreover, bdellovibrios could completely consume layers of other bacterial prey at hydrated solid−air interfaces.[13]

AFM revealed many details of the *Bdellovibrio* life cycle and the structure of the bdelloplast on the nanometer-to-micrometer scale.[13] Whereas uninvaded *E. coli* prey cells are characteristically rod-shaped with dimensions of roughly 0.75 μm × 2 μm, the bdelloplasts derived from the *E. coli* prey cells have a distinctly round shape with a diameter of roughly 1.5 μm. Bdelloplasts are also smoother than uninvaded *E. coli* when imaged in air. *E. coli* have a wrinkled appearance in air that is thought to be due to a contraction of the periplasm on drying that causes the outer membrane and peptidoglycan to shrink over the cytoplasmic membrane,[21] but bdelloplasts do not.[13] On the basis of how the tip interacted with the sample during imaging, producing occasional streaks and artifacts, we hypothesized that the bdelloplasts are stickier and more hydrophobic than the native prey cells.[13]

Our previous AFM measurements on bdellovibrios were performed in air, but it is unknown what effect drying might have on the surfaces of these cells. Though there are significant challenges to imaging cells in fluid using AFM, several groups have produced bacterial images showing nanoscale variations in the surface and cellular structures such as pili and flagella.[22,23] Furthermore, it is challenging to perform useful physical measurements on bacterial cell surfaces in air because of complicating capillary forces between the tip and the surface.[23,24] In fluid, it is possible not only to observe the bacterial cell surface but also to probe its physical properties: AFM force curves have been used to evaluate both the elasticity and adhesion of bacterial cells as the tip is extended to them and retracted.[25–33] In this work, we describe the physical changes that occur in *E. coli* prey cells as they are consumed by the bacterial predator *Bdellovibrio bacteriovorus* 109J. Notably, we utilize a biofilm-forming *E. coli* prey strain that adheres strongly and naturally to a glass surface, allowing us to make AFM measurements on native prey cells in fluid without chemically altering the bacteria. Traditional biochemical techniques have shown that bdellovibrios extensively modify the prey cell wall and cytoplasmic membrane during their "growth phase" inside of their prey, but little is known about the physical changes that result from these biochemical processes.[3,4,6,34–39] Here we use AFM imaging and force measurements to demonstrate that the *Bdellovibrio*-induced biochemical modifications cause major changes in the elasticity and adhesive properties of *E. coli* prey cells.

Materials and Methods

Media and Buffers. Nutrient broth (NB) consists of 8 g of Difco nutrient broth, 1 g of yeast extract, and 5 g of casamino acids per liter of H_2O. Dilute nutrient broth (DNB) consists of 0.8 g of Difco nutrient broth, 0.1 g of yeast extract, and 0.5 g of casamino acids per liter of H_2O. DNB was supplemented with 0.1 mM $MgCl_2$ and 1 mM $CaCl_2$. HEPES−metals buffer (HM) consists of 10 mM HEPES buffer, 0.1 mM $MgCl_2$, and 1 mM $CaCl_2$. The HM buffer was amended as necessary with varying amounts of NaCl.

Bacterial Cell Cultures. *E. coli* ZK1056, provided by Dr. Roberto Kolter and Dr. Mark Martin, was grown to saturation overnight in NB at 37 °C (to approximately 10^9 cells/mL). *E. coli* ZK1056 cells were pelleted by centrifugation, resuspended in an equal volume of 25% glycerol in DNB, aliquotted into 1.7 mL Eppendorf tubes, and frozen at −20 °C until use (generally within 1 week).

Bdellovibrio bacteriovorus 109J was obtained from the American Type Culture Collection (no. 15143, Manassas, VA) and was propagated in two-membered liquid growth cultures on *E. coli* ZK1056.[1,13,14] The two-membered growth cultures were grown in 50 mL of DNB at 30 °C with shaking for 5 days until the bdellovibrios reached their maximum concentration.[40] The cultures were then filtered through cellulose syringe filters (0.45 μM pore size, Fisher Scientific) to separate the smaller *Bdellovibrio* predator cells from the larger *E. coli* 1056 prey cells. The filtrate containing *Bdellovibrio* cells was supplemented with 25% glycerol, divided into aliquots and place in Eppendorf tubes, and frozen at −20 °C until use within 1 week.

Mixed-species cultures were prepared by first growing *E. coli* ZK1056 cells to saturation in NB at 37 °C for 1 day (to approximately 10^9 cells/mL). Five milliliters of this *E. coli* ZK1056 culture was diluted with sterile water to 50 mL total volume, and 100 μL of concentrated, filtered *Bdellovibrio* stock culture was added.[40] The 50 mL mixed culture was incubated with shaking in a sterile 500 mL Erlenmeyer flask at 30 °C for 48 h. At this point, the culture contained a mixture of healthy *E. coli* ZK1056, *Bdellovibrio* predators,

(13) Núñez, M.; Martin, M. O.; Duong, L.; Ly, E.; Spain, E. *Biophys. J.* **2003**, *84*, 3379–3388.
(14) Núñez, M. E.; Martin, M. O.; Chan, P. H.; Spain, E. M. *Colloids Surf., B* **2005**, *42*, 263–271.
(15) Núñez, M. E.; Martin, M. O.; Chan, P. H.; Duong, L. K.; Sindhurakar, A. R.; Spain, E. M. *Methods Enzymol.* **2005**, *397*, 256–268.
(16) O'Toole, G.; Kaplan, H. B.; Kolter, R. *Annu. Rev. Microbiol.* **2000**, *54*, 49–79.
(17) Watnick, P.; Kolter, R. *J. Bact.* **2000**, *182*, 2675–2679.
(18) Parsek, M. R.; Singh, P. K. *Annu. Rev. Microbiol.* **2003**, *57*, 677–701.
(19) Stoodley, P.; Sauer, K.; Davies, D. G.; Costerton, J. W. *Annu. Rev. Microbiol.* **2002**, *56*, 187–209.
(20) Costerton, J. W.; Lewandowski, Z.; Caldwell, D. E.; Korber, D. R.; Lappin-Scott, H. M. *Annu. Rev. Microbiol.* **1995**, *49*, 711–745.
(21) Umeda, A.; Saito, M.; Amako, K. *Microbiol. Immunol.* **1998**, *42*, 159–164.
(22) Dufrêne, Y. F. *J. Bacteriol.* **2002**, *184*, 5205–5213.
(23) Alessandrini, A.; Facci, P. *Meas. Sci. Technol.* **2005**, *16*, R65−R92.
(24) Xu, L.; Lio, A.; Hu, J.; Ogletree, D. F.; Salmerom, M. *J. Phys. Chem. B* **1998**, *102*, 540–548.
(25) Dague, E.; Alsteens, D.; Latge, J.-P.; Verbelen, C.; Raze, D.; Baulard, A. R.; Dufrêne, Y. F. *Nano Lett.* **2007**, *7*, 3026–3030.
(26) Yao, X.; Walter, J.; Burke, S.; Stewart, S.; Jericho, M. H.; Pink, D.; Hunter, R.; Beveridge, T. J. *Colloids Surf., B* **2002**, *23*, 213–230.
(27) van der Mei, H. C.; Busscher, H. J.; Bos, R.; de Vries, J.; Boonaert, C. J. P.; Dufrêne, Y. F. *Biophys. J.* **2000**, *78*, 2668–2674.
(28) Razatos, A.; Ong, Y.-L.; Sharma, M. M.; Georgiou, G. *Proc. Natl. Acad. Sci. U.S.A.* **1998**, *95*, 11059–11064.
(29) Velegol, S. B.; Logan, B. E. *Langmuir* **2002**, *18*, 5256–5262.
(30) Camesano, T. A.; Logan, B. E. *Environ. Sci. Technol.* **2000**, *34*, 3354–3362.
(31) Arnoldi, M.; Fritz, M.; Baurlein, E.; Radmacher, M.; Sackmann, E.; Boulbitch, A. *Phys. Rev. E* **2000**, *62*, 1034–1044.
(32) Arnoldi; M., K. C.; Baurlein, E.; Radmacher, M.; Fritz, M. *Appl. Phys. A: Mater. Sci. Process.* **1998**, *66*, S613–S617.
(33) Abu-Lail, N. I.; Camesano, T. A. *Langmuir* **2002**, 7296–7301.
(34) Kuenen, J. G.; Rittenberg, S. C. *J. Bacteriol.* **1975**, *121*, 1145–1157.
(35) Thomashow, M. F.; Rittenberg, S. C. *J. Bacteriol.* **1978**, *135*, 998–1007.
(36) Thomashow, M. F.; Rittenberg, S. C. *J. Bacteriol.* **1978**, *135*, 1008–1014.
(37) Thomashow, M. F.; Rittenberg, S. C. *J. Bacteriol.* **1978**, *135*, 1015–1023.
(38) Nelson, D. R.; Rittenberg, S. C. *J. Bacteriol.* **1981**, *147*, 860–868.
(39) Odelson, D. A.; Patterson, M. A.; Hespell, R. B. *J. Bacteriol.* **1982**, *151*, 756–763.
(40) Because they have a long life cycle and need be cultured on other organisms, the concentration of *Bdellovibrios* in a given solution is difficult to determine.[1,14]

and bdelloplasts.[14] The culture was then centrifuged, the pellet containing all three kinds of cells was resuspended in the same volume of 25% sterile glycerol, and the cells were frozen in aliquots at −20 °C. This mixed culture was used to inoculate 24-well plates to form mixed-species biofilms.

Biofilms. These were prepared by the addition of 25 μL of either single-species or mixed-stock cultures to 1100 μL of DNB in each well of a sterile 24-well plate. As described previously, each well also contained an upright, sterile, circular glass coverslip submerged halfway in the growth medium, upon which a visible biofilm formed at the air−liquid interface.[14,15] The cultures in these 24-well plates were allowed to grow for 2 days prior to removal of the glass coverslips for imaging. The glass coverslips were gently rinsed five times in sterile water to remove excess salts and loose bacteria. The coverslip was then glued to a glass slide with either of the equivalent sides facing up and was moved immediately to the AFM. The cells remained covered in either growth medium, water, or HM buffer throughout the duration of sample preparation and AFM imaging and were never allowed to dry out.

Although single-species *E. coli* ZK1056 cultures were grown and imaged to establish experimental parameters and obtain biofilm images, all height and force measurements reported here were made within the mixed-species biofilms on either infected or uninfected *E. coli* ZK1056 cells to confirm that all experimental parameters were identical. Forty-eight hours after establishment, the mixed-culture biofilms contained a mixture of uninvaded *E. coli* ZK1056, relatively rare bdelloplasts, and *Bdellovibrio* predators.[14] Cells were identified as uninvaded or invaded by characteristic shape and by the presence or absence of the growing *Bdellovibrio* predator inside. At least 30 separate mixed-culture biofilms were investigated by AFM, all prepared from the same initial mixed liquid culture to maintain the same initial concentrations of prey and predator cells.[40] Because 2-day-old biofilms are relatively simple and undifferentiated, the appearance of the biofilm as a whole and of individual cells was consistent from biofilm to biofilm.

AFM Instrumental Parameters. Images were obtained using an Asylum Research (Santa Barbara, CA) MFP-3D AFM in Alternating Current (AC) mode. The scan rate was kept at 0.25 Hz while all other parameters were optimized for imaging. Cells were imaged in aqueous HM buffer, a solution in which bdellovibrios are known to remain viable.[1] Cells were kept covered in buffer during imaging. The shorter, narrow cantilevers on silicon nitride probes (DNP-S, Veeco Instruments, Santa Barbara, CA), which have a nominal spring constant of 0.32 N/m, were used for all experiments.

Cell heights were determined from the biofilm images. Because the measured heights can depend on the applied force, the amplitude was kept as constant as possible between scans. Also, bdelloplast heights were measured in the same biofilm and with the same tip as uninfected prey cell heights. Wherever possible, these heights were measured side-by-side on the same scanned image with uninfected prey cells. Cell heights were determined from the images of 71 different cells under various conditions. Three or four cross-sections were taken of each cell, crossing the cell in different directions parallel, perpendicular, and at an angle to the scan direction, and the height from the glass slide to the highest point on the cell was determined for each cross-section. All of these heights were included in the data analysis. The average and standard errors were determined for each set, and a Student's *t* test was used to evaluate the significance of the differences between uninvaded *E. coli* ZK1056 cells and bdelloplasts at each salt concentration.

Once an uninfected *E. coli* ZK1056 cell or an infected bdelloplast was identified using the imaging mode, locations at which to take force data were selected. Locations were usually chosen toward the center of the cell to avoid edge effects and tip displacement due to hysteresis, and at least 10 curves were acquired at each location. The force distance was set such that the tip would be completely out of contact with the cell when it was withdrawn (3.14 um). The scan speed was set to 0.48 Hz. The large applied force (equivalent to 25 nN) was chosen such that the extent of the nonlinear region and the slope of the linear region of the bdelloplast curves could be identified unequivocally. After force curve acquisition was completed, a second image was obtained to make sure that the cell had not shifted, ruptured, become dislodged, or been otherwise damaged. Force curves were obtained on cell-free areas before and after taking measurements on cells to make sure that contact with the cells did not alter the properties of the tip.

Image and Force Curve Processing. Once images were obtained, they were flattened and cropped using Igor Pro software for MFP-3D. Images were then imported into Adobe Photoshop, where scale bars were added but no further modifications were made. Force curves were also processed using Igor Pro MFP-3D software.

To quantify cell elasticity, nominal cellular spring constants were determined by modeling the cell−tip interaction as two springs.[29,41] $k_{\text{cantilever}}$ was determined for each cantilever using a clean glass slide in HM buffer and a single force curve and was rechecked after cell measurements were made to confirm the integrity of the tip. The thermal method was used to determine the spring constant, as built into the MFP-3D software. We first determined the sensitivity of the cantilever by bringing it into contact with a hard surface to calibrate which deflection corresponds to which *z* distance. We then performed thermal tuning to determine the cantilever's resonance frequency, which allowed an algorithm to compute the spring constant using the equipartition theory.[42] For each individual force curve, the slope of the linear region of the force curve taken on a cell ($k_{\text{effective}}$) was used with eq 1

$$1/k_{\text{effective}} = 1/k_{\text{cell}} + 1/k_{\text{cantilever}} \quad (1)$$

and the $k_{\text{cantilever}}$ values specific to that data set to determine k_{cell}.[29,41] Once k_{cell} was determined for every force curve ($n = 1771$), the averages and standard errors were calculated. A Student's *t* test was used to evaluate the significance of the differences between uninvaded *E. coli* ZK1056 cells and bdelloplasts at each ionic strength.

Because there were three regimes for the extension curves for all of the cells (the flat approach, the nonlinear compression, and the linear compression), both $k_{\text{effective}}$ and $(\Delta X, \Delta F)_{\text{nonlinear}}$ were determined. The linear regime was determined by extrapolating a straight line along the extension curve from the high-force region toward lower force. A second flat horizontal line was drawn along the approach region, and the portion of the curve that did not conform to either of the two lines was defined as the nonlinear region. The adhesion events measured from the retraction curves represent the difference in force between each vertical displacement as a function of the distance from the cell surface where the jump occurred $(\Delta X, \Delta F)_{\text{adhesion}}$. Once the $(\Delta X, \Delta F)_{\text{nonlinear}}$ or $(\Delta X, \Delta F)_{\text{adhesion}}$ was determined for every extension or retraction curve, the averages and standard errors were calculated. A Student's *t* test was used to evaluate the significance of the differences between uninvaded *E. coli* ZK1056 cells and bdelloplasts at each ionic strength.

Results

Imaging Prey Cell Biofilms and Bdelloplasts. To establish our AFM imaging parameters, we examined simple *E. coli* ZK1056 biofilms on glass coverslips. Figure 2 shows representative images from those biofilms in HEPES buffer with $MgCl_2$ and $CaCl_2$ (HM). Depending on the scan size and what part of the biofilm was imaged, *E. coli* ZK1056 cells were imaged in communities (as in Figure 2A−C) or individually (as in Figure 2D). The cells were firm and had an average height of around 400 nm (vide infra). Many images revealed EPS (exopolysaccharides, or more generally, exopolymeric substances) visible around the bacteria. However, we found that images of *E. coli* ZK1056 biofilms obtained in fluid were generally less well resolved than images of the same biofilms obtained in air.[14]

After optimizing the parameters needed for imaging the *E. coli* ZK1056 biofilm, we imaged mixed biofilms of *Bdellovibrio bacteriovorus 109J* and *E. coli ZK 1056*. When the mixed biofilm

(41) Burks, G. A.; Velegol, S. B.; Paramonova, E.; Lindenmuth, B. E.; Feick, J. D.; Logan, B. E. *Langmuir* **2003**, *19*, 2366–2371.
(42) Hutter, J. L.; Bechhoefer, J. *Rev. Sci. Instrum.* **1993**, *64*, 1868–1873.

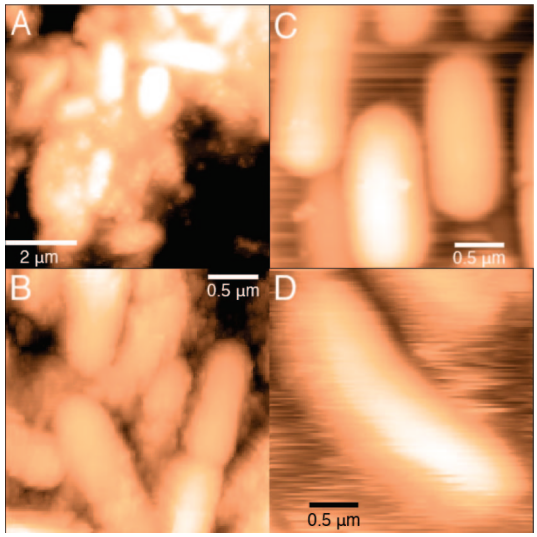

Figure 2. *E. coli* ZK1056 biofilms imaged in HM buffer without chemical fixation. (A) Height image of an active biofilm with many *E. coli* ZK1056 growing and dividing. The image has a height scale (z dimension) of 500 nm. (B) Height image on *E. coli* growing in a biofilm. The height scale is 450 nm. (C) Height image of three *E. coli* ZK1056 cells with a z scale of 500 nm. (C) Height image of a single *E. coli* ZK1056 cell. The height scale is 450 nm. In panels A and B, the EPS (exopolysaccharides or exopolymeric substances) secreted by the biofilm cells are visible as darker, fluffy "clouds" around the edges of the cells.

samples containing bdellovibrios are viewed in a phase-contrast light microscope or using the visual system of the MFP-3D AFM, we observe free-swimming bdellovibrios in the medium. This evidence confirms that the *Bdellovibrio bacteriovorus* 109J population is alive and actively hunting in the sample. We were unable to image attack-phase bdellovibrios using AFM because they are motile in the attack phase and do not remain fixed to the surface. However, imaging the biofilm with the AFM exposes the presence of bdelloplasts, invaded prey cells with predators growing in them. The bdelloplasts are distinctly round in shape, making them readily identifiable. When the bdelloplasts are viewed individually on a smaller scale, as in Figure 3, it is often possible to see details such as the *Bdellovibrio* growing inside the prey cell.

A quantitative comparison of the height of uninvaded prey cells and bdelloplasts illustrates that bdelloplasts are significantly shorter than uninvaded *E. coli* cells when imaged in HM buffer (Figure 4). As the ionic strength of the medium increases, the heights of both the bdelloplasts and *E. coli* decrease. Notably, the bdelloplasts are always shorter than the *E. coli* regardless of ionic strength conditions (within >99% confidence intervals at each ionic strength).

Cell Elasticity. Force curves can reveal a great deal of useful information about the physical properties of a cell. The extension half of the force cycle reflects the advance of the tip toward the cell, the initial contact with the cell, and the deflection of the tip as it is pressed into the surface. The slope of the curve as the tip is deflected, $k_{\text{effective}}$, is used in eq 1 to determine the spring constant of the cell, k_{cell}, equivalent to the stiffness of the cell. The retraction curve, the second half of the force curve where the tip pulls away from the cell, is used to examine the adhesion events that occur between the tip and the cell surface.

Force measurements were obtained at several locations across the biofilms. The shape and slope of the extension curve are dependent on the sample surface. The extension curve for the glass substrate probed under fluid contains two regimes, a flat horizontal approach and a steep linear deflection (Figure 5A). The transition between these two regions is sharp. The extension curve on the *E. coli* ZK1056 cells has a less steep linear deflection than on glass (Figure 5B). The *E. coli* ZK1056 extension curve also can be separated into three regimes. Between the horizontal approach and the linear deflection, at the point at which the tip first contacts the *E. coli* ZK1056 cell, is a small nonlinear transition. The linear deflection in the bdelloplast curve has a less steep slope than either glass or the uninvaded *E. coli* ZK1056 prey cell (Figure 5C). The extension curve for the bdelloplast also has three regimes, much like the *E. coli* ZK1056 curve, but the nonlinear deflection in the bdelloplast extension curve is much larger than in the *E. coli* ZK1056 cells. The linear and nonlinear regimes were treated separately for the purposes of data analysis.

The slope of the linear portion of each extension curve was used to determine the stiffness of the cell, expressed as the average spring constant (Figure 6). In HM buffer, the bdelloplasts have an average spring constant of 0.064 ± 0.001 N/m, and the *E. coli* have an average spring constant of 0.23 ± 0.02 N/m, clearly indicating that the *E. coli* cells are stiffer than the bdelloplasts. To demonstrate that the observed spring constants reflect cell turgor pressure rather than membrane stiffness, spring constants for prey and bdelloplasts were measured at a variety of ionic strengths. As can be seen from Figures 4 and 6, as the ionic strength was increased and the height of the cells decreased, the spring constant of both *E. coli* ZK1065 cells and bdelloplasts decreased. Interestingly, the spring constants of both the *E. coli* and bdelloplasts decrease considerably between 0 and 25 mM NaCl added. The cells that were imaged in buffer with 50, 75, and 150 mM NaCl have progressively smaller spring constants, but the differences are less pronounced than after the first addition of NaCl to the buffer, indicating that the cell stiffness responds nonlinearly to the increase in ionic strength (Figure 1 in Supporting Information). On bdelloplasts in higher-ionic-strength media, a fourth region appeared in the extension curve at the highest distances and at forces with a slope identical to that of glass (data not shown). Because this region clearly corresponded to the substratum, it was not included in the analysis.

The force and distance components of the nonlinear regime between the approach to the cell surface and the linear deflection were measured for hundreds of extension curves (Figure 7). In the bdelloplast force curves, this large nonlinear region encompasses an average distance of approximately 300 ± 2.7 nm and an average force of 3.3 ± 0.04 nN ($n = 583$). The nonlinear region in the *E. coli* ZK1056 extension curves is significantly smaller than in the bdelloplast curves, both in terms of distance and force (Δdistance $= 12 \pm 0.4$ nm, Δforce $= 0.19 \pm 0.0087$ nN, and $n = 100$; Figure 7C). The nonlinear regime in the extension curves of bdelloplasts exposed to higher ionic strengths is smaller than in HM buffer (data not shown).

Adhesion. Adhesion is measured from the retraction half of the force cycle. Figure 8 shows representative adhesion events that were measured between the tip and bdelloplast or the tip and *E. coli*. The jagged teeth result from each snap-off or adhesion event. Note that each adhesion curve has a different, individual pattern of adhesion events. Overall, it is apparent by visual inspection that the force component of the adhesion events in the bdelloplast retraction curves are generally larger than the force component of the *E. coli* ZK1056 adhesion events.

The adhesion events were quantified by determining the difference in force between each vertical displacement as a function of the distance from the cell surface where the jump occurred. These force−distance pairs $(\Delta X, \Delta F)_{\text{adhesion}}$ are shown in Figure 9. Very little adhesion is measured between the tip and

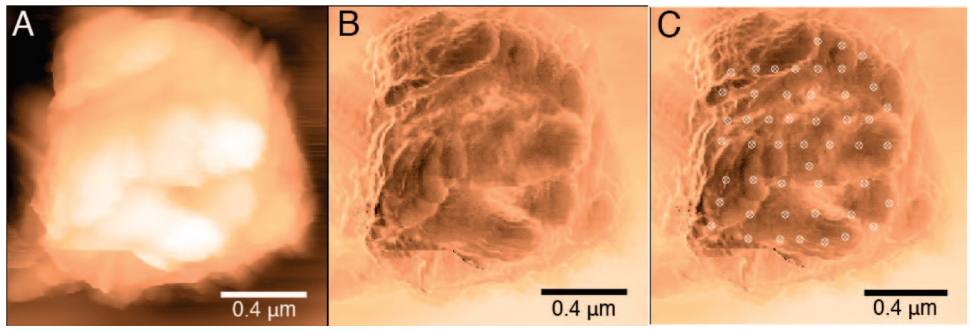

Figure 3. Bdelloplast imaged in HM buffer without chemical fixation. In contrast to the oblong, relatively smooth uninvaded *E. coli* ZK1056 prey cells seen in Figure 2, the bdelloplasts are round and rough. (A) Height image with a z scale of 400 nm. The growing *Bdellovibrio* predator is the c-shaped wormlike object in the center of the image. It is lighter in color than the rest of the image because it is the tallest part of the image. (B) Phase image with a θ scale of 20°. (C) Phase image with circles to indicate the positions where force curve data were collected. Force curves near the edges of the cell were collected but not used in the data analysis.

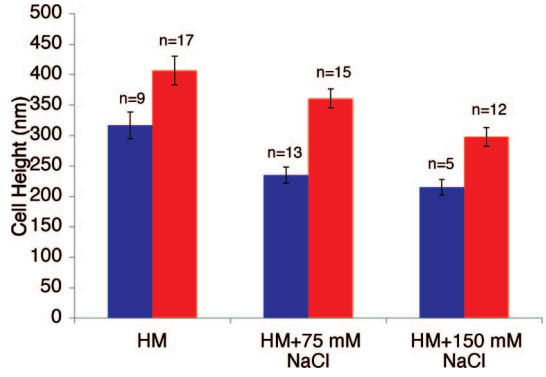

Figure 4. Average cell heights imaged in three solutions with different ionic strengths. The *E. coli* ZK1056 height is shown in red, and the bdelloplast height is shown in blue. Both types of cells decrease in height as the ionic strength increases, but the bdelloplasts always have a lower average height than *E. coli* ZK1056. The error bars represent the standard error for each data set. n is equal to the number of cells measured, where each cell was measured three to four times in different locations from cross-sections taken in different directions. (The probabilities that the heights of uninvaded cells and bdelloplasts are the same by the Student's t test are $P_{HM} = 0.0075$, $P_{HM+75\ mM\ NaCl} = 5.56 \times 10^{-9}$, $P_{HM+150\ mM\ NaCl} = 5.40 \times 10^{-5}$.)

glass (green). The distance ranges of adhesion measurements for bdelloplasts (blue) and *E. coli* ZK1056 (red) overlap extensively, but many of the bdelloplast adhesion events have larger pull-off forces than the *E. coli* ZK1056 adhesion events. As the ionic strength increases, the large-force adhesion events that characterize the bdelloplast force curves in buffer disappear (Figures 2 and 3 in Supporting Information). To quantify the specific and nonspecific contributions to the adhesion data, force distance pairs $(\Delta X, \Delta F)_{adhesion}$ were evaluated by Poisson analysis per Abu-Lail and Camesano,[33] but neither *E. coli* nor bdelloplast adhesion events could be fit to this model.

Discussion

Imaging Bacteria in Buffer. In this work, we imaged by AFM a biofilm-forming strain of *E. coli* bacterial cells in aqueous buffer without any chemical modification. To image the *Bdellovibrio* predators and prey by AFM, the cells must stick to a surface. Unfortunately, many laboratory strains of bacteria do not adhere strongly to surfaces, so previous investigators have imaged their bacterial cells in fluid by chemically bonding them to a surface. We avoided chemical fixation because of potential interference with subtle *Bdellovibrio*-induced physical changes occurring in the outer membrane of the bdelloplast. To image in aqueous buffer without chemically modifying the bacteria, we used as our prey biofilm-forming *E. coli* strain ZK1056, which adheres strongly and natively to glass in a fluid medium and forms simple bacterial biofilms at the air/fluid interface. *Bdellovibrio bacteriovorus* 109J can successfully prey on cells in these biofilms.[14] In aqueous buffer, we could clearly identify individual *E. coli* ZK1056 cells as well as *E. coli* ZK1056 living in groups characteristic of simple biofilm communities (Figure 2). Unlike gram-negative cells imaged in air,[21] the biofilm cells do not appear to be wrinkled in aqueous buffer. The EPS, outer membrane, and peptidoglycan remain hydrated, presenting a smooth surface to the tip. When voracious *Bdellovibrio* predators were added to the biofilm community, they attacked and consumed prey cells in the biofilm, as evidenced by the presence of bdelloplasts. We cannot directly probe the *Bdellovibrio* predator using AFM because it is either free-swimming or encased in its prey throughout its life cycle. As a result, we concentrated on elucidating the physical changes that occur in the *E. coli* ZK1056 prey cells when they are attacked, killed, and consumed by the predator. This work illustrates that interesting microbial systems can be investigated by AFM in a completely native state.

Biochemistry of the Bdelloplast. These AFM observations are particularly interesting because we can compare our physical measurements to what is known about the biochemistry of the bdelloplast. A *Bdellovibrio* predator uses a combination of mechanical forces and enzymatic activities to burrow into its gram-negative prey cell.[1–4] Initially, it produces a glycanase to locally weaken the outer membrane lipopolysaccharide (LPS) and the peptidoglycan, facilitating its entry into the periplasm.[35] It simultaneously produces a protease to weaken the peptidoglycan. These activities contribute to the characteristic "rounding up" of the bdelloplast. However, shortly after it enters the periplasm, it N-deacetylates the peptidoglycan amino sugars, effectively inactivating the glycanase and preventing further degradation of the peptidoglycan until the end of the invasion cycle.[36] Presumably to stabilize the outer "shell" of the bdelloplast and perhaps to dissuade other predators from attacking, it continues to modify the peptidoglycan and the outer membrane by removing the Braun lipoprotein, modifying the diaminopimelic acid component, and adding a fatty acid to the peptidoglycan.[36,37] It is unclear to what extent the *Bdellovibrio* invader modifies the outer membrane protein contingent,[31,43–45] but it does scavenge fatty acids and lipid A components for its own growing cell wall.[34,38] The prey's inner membrane does not escape remodeling;

(43) Tudor, J. J.; Karp, M. A. *J. Bacteriol.* **1994**, *176*, 948–952.
(44) Talley, B. G.; McDade, J.; Ralph, L.; Diedrich, D. L. *J. Bacteriol.* **1987**, *169*, 694–698.
(45) Diedrich, D. L.; Duran, C. P.; Conti, S. F. *J. Bacteriol.* **1984**, *159*, 329–334.

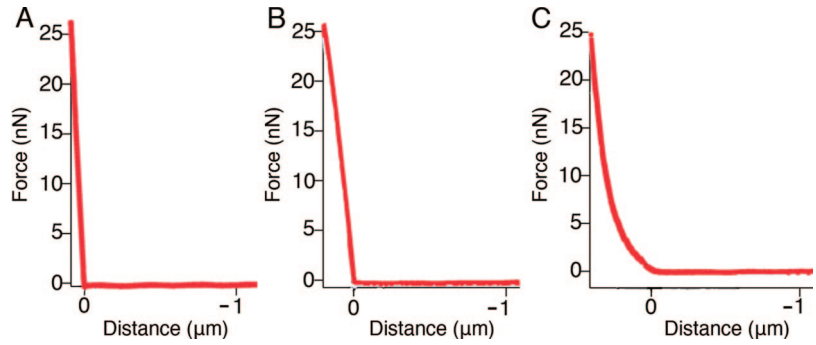

Figure 5. Examples of the extension portion of force curves measured on cells imaged in HM buffer. (A) Extension curve taken on glass. (B) Extension curve taken on an *E. coli* ZK1056 cell. (C) Extension curve taken on a bdelloplast. The 0 μm extension is defined as the point at which the tip is initially deflected.

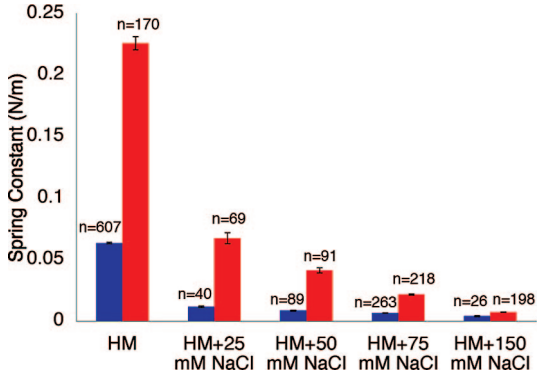

Figure 6. Average cell elasticity calculated as the spring constants of bdelloplasts (blue) and *E. coli* ZK1056 cells (red) in five solutions with increasing ionic strength. The elasticity was measured in HM buffer (HEPES buffer with $MgCl_2$ and $CaCl_2$) with varying amounts of NaCl between 0−150 mM. As the ionic strength was increased, the spring constants for *E. coli* ZK1056 and bdelloplasts decreased, but at all salt concentrations, bdelloplasts had a lower average spring constant than did *E. coli* ZK1056. The error bars represent the standard error of each data set; n is equal to the number of force curves analyzed. (The probabilities that uninvaded cells and bdelloplasts have the same spring constant by the Student's t test are $P_{HM} = 1.19 \times 10^{-102}$, $P_{HM+25\ mM\ NaCl} = 4.89 \times 10^{-16}$, $P_{HM+50\ mM\ NaCl} = 4.52 \times 10^{-42}$, $P_{HM+75\ mM\ NaCl} = 1.35 \times 10^{-99}$, and $P_{HM+150\ mM\ NaCl} = 7.09 \times 10^{-7}$.)

it becomes so leaky as to present no barrier to the *Bdellovibrio*'s uptake of its prey's cytoplasmic contents.[46,47]

Differences in the Shape and Height of the Prey Cell and Bdelloplast. How then do the physical changes that we measure by AFM correspond to the biochemical changes that occur in the bdelloplast described previously? First and foremost, the AFM images clearly illustrate the rounded shape of the bdelloplasts. The changes in the prey cell shape that are readily observed during AFM imaging are likely due to the loss of peptidoglycan cross-linking as the *Bdellovibrio* first invades its prey. Without its stiff peptidoglycan layer, the invaded *E. coli* is unable to maintain its rodlike shape and thus rounds up early in the invasion process.

The average height measured for the uninvaded *E. coli* ZK1056 cells is larger than for the bdelloplasts (Figure 4). A smaller bdelloplast height initially seems odd given that the *Bdellovibrio* predator is squeezed into the bdelloplast along with the contents of the prey cell. However, shorter bdelloplasts are consistent with our previous observations in air[13,14] and can be explained in the context of bdelloplast biochemistry. Some of this loss of height of the *E. coli* cells after invasion by the predator may be due to "sagging" from the breakdown of the peptidoglycan,[35,36] whereas some of the loss in height is probably due to a loss of turgor pressure and/or cell volume.[6,35] It is important to note that because the heights are measured using a scanning probe that physically interacts with the cell surface, the differences in height between the softer bdelloplasts and the stiffer *E. coli* ZK1056 cells may be somewhat exaggerated. However, the bdelloplasts clearly are shorter than the *E. coli* ZK1056 cells because even when they are imaged side-by-side in the same scan with a minimum amount of applied force the bdelloplasts are noticeably shorter.

Elasticity, Spring Constants, and Turgor Pressure. We used the interaction of the tip as it is extended to probe the elasticity of bdelloplasts and uninvaded prey cells. Interestingly, we observed three regimes in the extension curves of both kinds of cells: a horizontal approach region, a nonlinear deflection, and a linear deflection. As discussed below, the nonlinear region corresponds to the initial contact between the tip and the cell surface polymers and the cell wall, whereas in the linear region the tip is pushing against the turgor pressure of the cellular contents. The nonlinear and linear deflection regimes were treated separately. Because the nonlinear region of the bdelloplast extension curve is so large, we chose an unusually high set point for the deflection limit of the cantilever so that we could clearly define the slope of the linear regime as well as the extent of the nonlinear regime $(\Delta X, \Delta F)_{nonlinear}$. For the sake of consistency, we used the same set point for bdelloplasts and *E. coli* ZK1056 cells. Although we were initially concerned that we might damage the cells by pushing so hard on them with sharp tips and relatively stiff cantilevers, images of cells before and after force measurements show no signs of damage, and the first force curves taken on cells are the same as later ones. In the higher-ionic-strength media, the advancing tip occasionally distorted and/or penetrated the shorter, softer bdelloplasts such that that the tip could directly probe the glass substratum at its furthest extension. In this case, a fourth region appeared in the extension curve at the farthest distances and for forces with a slope identical to that of glass (data not shown). Because this region clearly corresponded to the glass, it was not included in the analysis.

The ionic strength dependence of the spring constants (determined from the linear portion of the extension curve) confirms that k_{cell} reflects cell turgor pressures.[26,31,32] As the ionic strength outside the cell is increased, water diffuses out of the cell, decreasing the cell volume and making the cell shorter, smaller, and softer. Thus, if the spring constants *decrease* with increasing ionic strength, then the linear portion of the curve reflects turgor pressure.[26,31,32] However, increasing the ionic

(46) Rosson, R.; Rittenberg, S. C. *J. Bacteriol.* **1979**, *140*, 620–633.
(47) Ruby, E. G.; McCabe, J. B.; Barke, J. I. *J. Bacteriol.* **1985**, *163*, 1087–1094.

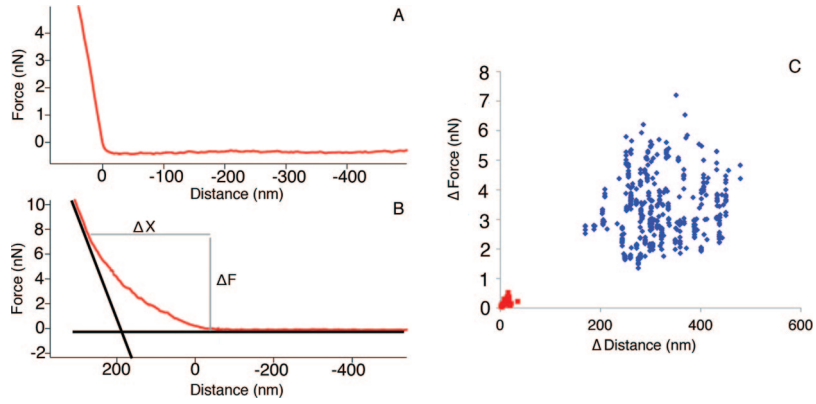

Figure 7. Measurements of the nonlinear region of the extension portion of the force cycles. (A) Representative extension curve taken on an *E. coli* ZK1056 cell. (B) Representative extension curve taken on a bdelloplast with the nonlinear region highlighted. The nonlinear region of the bdelloplast extension curve is much larger than that of the *E. coli* ZK1056. (C) The plot of the $(\Delta X, \Delta F)_{\text{nonlinear}}$ pairs for force curves taken on *E. coli* ZK1056 cells (red) and bdelloplasts (blue) shows that the bdelloplast nonlinear region contains larger changes in both force and distance than does the nonlinear region in the *E. coli* ZK1056 extension curve. (The probabilities that the adhesion of uninvaded cells and bdelloplasts are the same by the Student's *t* test are $P_{\text{force}} = 4.27 \times 10^{-19}$ and $P_{\text{distance}} = 1.95 \times 10^{-204}$.)

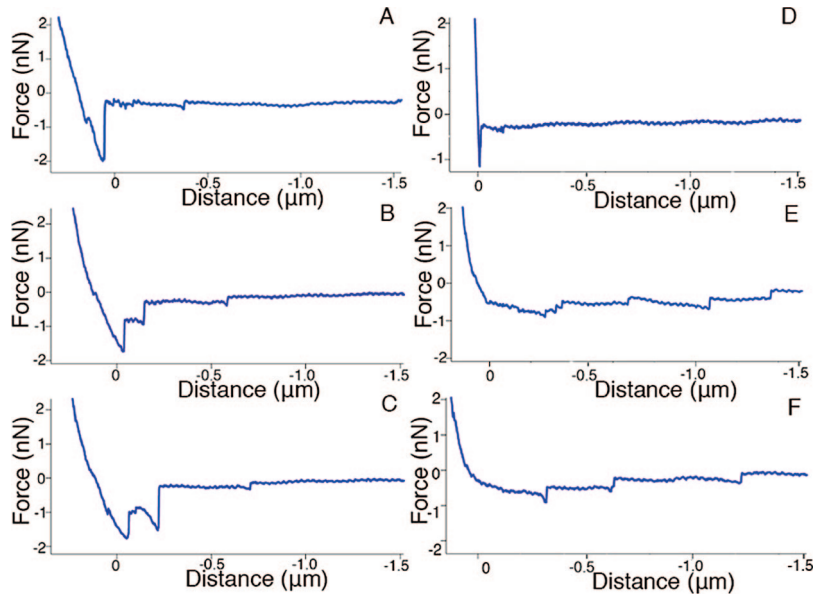

Figure 8. Representative retraction curve of the force cycle. (A−C) Bdelloplast retraction curves showing multiple adhesion events. (D−F) *E. coli* ZK1056 retraction curves showing multiple adhesion events. The 0 μm distance is defined as the point on the extension curve at which the tip is initially deflected.

strength causes a shielding of charged groups on the cell exterior, potentially leading to the compression of extracellular polymers and effective stiffening of the cell surface.[27,48,49] If the linear portion of the curve reflected interactions of the tip with cell surface polymers, then we would expect the spring constants to *increase* with increasing ionic strength. The fact that the measured spring constants decrease with increasing ionic strength confirms that our spring constants reflect the turgor pressure of the bacterial cells rather than the stiffness of the cell wall.

The spring constant that we measure for the uninvaded *E. coli* ZK1056, 0.23 N/m, is within the range of what has been previously observed for bacterial cells in fluid (reviewed in ref 50). Though our measured spring constant is at the high end of the range, differences in cell type, preparation technique, and the ionic strength of the medium may all contribute to this variety of spring constants that are reported. Indeed, Burks et al., Sullivan et al., and Yao et al. measured bacterial spring constants in low-ionic-strength buffers or water with a spring contstant of similar magnitude to our *E. coli* ZK1056 spring constant measured in low-ionic-strength HM buffer.[26,41,51] The spring constants that we measured for *E. coli* ZK1056 in higher-ionic-strength buffers are comparable to those reported in the literature for cells measured in growth medium.[50] Our measured spring constants would be somewhat lower if we were to treat the linear and nonlinear parts of the curve as a single regime, which would clearly be problematic for bdelloplasts in particular. Also, though the precision of our measurements of cellular spring constants is high as expressed by the small standard errors, the whole set of k_{cell} values depends on the determination of $k_{\text{cantilever}}$, which is accurate to within only 10−20%. For all of these reasons, a comparison of cellular spring constants between investigators, preparations, and cell types should be made with some caution, though we can say with confidence that *E.coli* ZK1056 cells have higher spring constants

(48) Camesano, T. A.; Abu-Lail, N. I. *Biomacromolecules* **2002**, *3*, 661–667.
(49) Dufrêne, Y. F. *Biophys. J.* **2000**, *78*, 3286–3291.
(50) Méndez-Vilas, A.; Gallardo-Moreno, A. M.; Gonzálas-Martin, M. L. *Microsci. Microanal.* **2007**, *13*, 55–64.
(51) Sullivan, C. J.; Venkataraman, S.; Retter, S. T.; Allison, D. P.; Doktycz, M. J. *Ultramicroscopy* **2007**, *107*, 934–942.

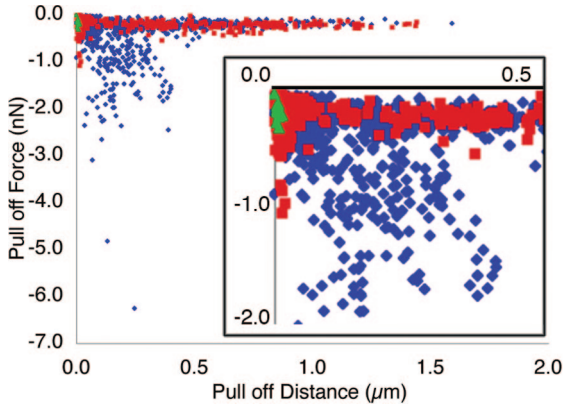

Figure 9. Plot of force and distance components to adhesion events for *E. coli* ZK1056, bdelloplast, and glass probed in HM buffer. Bdelloplast adhesion events are shown in blue, *E. coli* ZK1056 adhesion events are shown in red, and glass adhesion events are shown in green. Whereas there is overlap between all three sets, the bdelloplast set contains many more large pull-off forces than the *E. coli* ZK1056, as seen in the inset ($P_{distance} = 6.37 \times 10^{-14}$ and $P_{force} = 3.37 \times 10^{-9}$).

than bdelloplasts and that these values decrease with ionic strength.

The overall lower values of the spring constants measured for bdelloplasts as compared to those of the uninvaded prey cells reveal that the turgor pressure of bdelloplasts must be lower than those of the uninvaded prey cells. This lower turgor pressure in the bdelloplasts may be due in part to the major but transient disruption in cell wall integrity that occurs during *Bdellovibrio* penetration into the prey cell.[6,35] A loss of prey cell volume through the temporary outer membrane breach could explain both the lower spring constant and the lower cell height of the bdelloplast compared to those of the uninvaded prey cells. The difference in apparent cell stiffness may also be due to the redistribution of cytoplasmic material within the prey cell that occurs as the *Bdellovibrio* consumes its prey. The *Bdellovibrio* switches the osmotic barrier of the invaded prey cell from the cytoplasmic membrane to the outer membrane.[37] Disruption of the cytoplasmic membrane to release biomolecules for *Bdellovibrio* consumption may cause an apparent decrease in bdelloplast tugor pressure.

Strikingly, both uninvaded *E. coli* ZK1056 and bdelloplasts exhibit similar responses to changes in ionic strength (Figure 6), indicating that the diffusive barrier of the bdelloplast outer membrane is generally maintained. Preservation of the bdelloplast *outer* membrane integrity is well documented and is essential to the success of *Bdellovibrio* in scavenging nutrients from its prey.[52] On closer inspection, however, it is clear that the logarithmic response of the spring constant to increasing ionic strength is not in fact identical for *E. coli* cells and bdelloplasts (Figure 1 in Supporting Information). The *E. coli* ZK1056 cells are alive in our AFM preparations and can actively change their cell volumes and ionic compositions to respond to changes in the ionic strength of their surroundings, whereas the bdelloplasts (or at least the prey portions thereof) are dead and thus can respond to changes in ionic strength only via more passive mechanisms. As a result, it is not surprising that the spring constants of the two types of cells do not correlate identically with ionic strength.

Elasticity and Cell Surface Properties. The nonlinear portion of the extension force curves provides us with information about the cell wall and LPS of the prey cells and bdelloplasts. The nonlinear region of the extension curves has been described previously and has sometimes been referred to as the "repulsive" region.[26,28,30,53] A portion of this nonlinear deflection, particularly at short distances, can be caused by repulsive electrostatic and van der Waals forces between the cell surface and the tip, but much of the deflection at larger distances must be due to "steric" factors (i.e., the interaction between the tip and various soft polymeric biomolecules on the cell surface and in the cell wall[54]).

A small nonlinear transition is observed in the extension curves for the uninvaded prey *E. coli* ZK1065 as the tip is pushed into the cell (Figure 7). *E. coli* ZK1056 is a rough strain, meaning that it lacks an O-antigen component on its outer membrane LPS (data not shown). Thus, the change in the distance component (ΔX) of its small nonlinear transition (12 nm) corresponds approximately to the width of the rough LPS and phospholipids that make up the outer membrane (8−10 nm).[41] Having observed similar nonlinear regions in the extension force profiles of several *E. coli* rough strains, Velegol and Logan proposed that in the nonlinear regime the tip contacted the outer membrane but had yet to encounter the stiff peptidoglycan layer.[29]

In contrast, the nonlinear transition in the bdelloplast extension curves encompasses a much larger range both in distance and force than the nonlinear region in the *E. coli* ZK1056 curves. The change in distance over the nonlinear region in the bdelloplasts is on the order of 300 nm and as such is much greater than the width of the outer membrane. Though the *Bdellovibrio* predator does modify the outer membrane of the bdelloplast inside of which it is growing, it is extremely unlikely that *Bdellovibrio* adds 300-nm-long molecules to the surface of the bdelloplast.[1,13,14,34,38,55,56] Instead, this difference between the extension curves for the two kinds of cells indicates that the tip−cell interaction is significantly different for the bdelloplast as compared to that for the uninvaded cell. In these experiments, the tip is extended to a large force deflection set point, pushing a sharp tip and stiff cantilever hard up against the cells. As the growing predator extensively remodels the bdelloplast outer membrane and degrades the peptidoglycan, it weakens the integrity of this barrier to mechanical stress from the advancing tip. Thus as the tip is advanced, it is first likely to substantially deform and ultimately penetrate the bdelloplast cell wall before meeting resistance from the intracellular contents, bringing about the long-distance components in the nonlinear region of the extension curves.

Adhesion. On the basis of the adhesion events measured for bdelloplasts, *E. coli* ZK1056, and glass, it is clear that the bdelloplast interacts more strongly with the tip than does *E. coli* ZK1056 (Figure 9). Several factors could contribute to the large force adhesion events measured in the retraction curves of the bdelloplasts. Because of the relatively high forces, stiff cantilever, and sharp tip used in these experiments, and consistent with the large distance components of the bdelloplast extension curve, it is reasonable to assume that the tip penetrates the compromised cell wall/peptidoglycan of a bdelloplast. As a result, the tip will make contact with more biomolecules on the bdelloplast than on an uninvaded cell, which breaks with a correspondingly larger resulting force when the tip is withdrawn. Alternatively, the larger force measured between the bdelloplast and the tip may result from the predator's specific biochemical modifications of the prey cell's wall and peptidoglycan, exposing new functional groups to interact favorably with the tip that were not previously present. For example, the degraded, modified peptidoglycan may

(52) Cover, W. H.; Martinez, R. J.; Rittenberg, S. C. *J. Bacteriol.* **1984**, *157*, 385–390.
(53) Vadillo-Rodríguez, V.; Busscher, H. J.; Norde, W.; de Vries, J.; Dijkstra, R. J. B.; Stokroos, I.; van der Mei, H. C. *Appl. Environ. Microbiol.* **2004**, *70*, 5441–5446.
(54) Gaboriaud, F.; Dufrene, Y. F. *Colloids Surf., B* **2007**, *54*, 10–19.
(55) Burnham, J. C.; Hashimoto, T.; Conti, S. F. *J. Bacteriol.* **1968**, *96*, 1366–1381.
(56) Nelson, D. R.; Rittenberg, S. C. *J. Bacteriol.* **1981**, *147*, 869–874.

directly adhere to the tip. Biochemical investigations indicate that uncharged N-acetyl groups in the *E. coli* peptidoglycan are unmasked by the predator's enzymes.[36] These amino groups could be positively charged in the bdelloplast, allowing for stronger adhesion between the negatively charged silicon nitride tip and cell.

The distances over which both the tip−*E. coli* and tip−bdelloplast adhesion events occur are in the hundreds of nanometers and some are greater than a micrometer. These distances are long relative to adhesion data collected by other groups but not egregiously so: Abu-Lail and Camesano measured adhesion events between silicon nitride tips and *E. coli* with pull-off distances upwards of 600 nm,[33] and Vadillo-Rodríguez et al. measured adhesion events between the AFM tip and *Streptococcus mitis* up to 1186 nm.[57] The long-distance adhesion events that we measure are not artifacts of our retraction speed because either slower or faster retractions produce the same adhesion events (data not shown). A possible explanation is that EPS attaches to the tip as it is pulled away from the cell. We expect that there will be EPS readily available on the surface of both uninvaded *E. coli* ZK1056 and bdelloplasts because these biofilm-forming cells are imaged in a native state and though gently rinsed have been neither chemically fixed nor extensively processed. An alternate explanation is that pili adhere to the tip: if a pilus were to attach to the tip, then it might stretch to several hundred nanometers before the connection broke.[58] This adhesion to pili should be the same for both bdelloplasts and uninvaded *E. coli* and may explain some of the overlapping adhesion data that occurs. A third explanation for these long pull-off distances in the bdelloplasts is that cell wall degradation allows the tip to push further into the cell and draw out long pieces of degraded cell membrane or peptidoglycan.

As the ionic strength is increased, the adhesion events in the bdelloplast that are characterized by large forces disappear (Figures 2 and 3 in Supporting Information). Thus, these events appear to have an electrostatic component that disappears when the charged groups involved are screened by additional salt. At neutral pH, the bdelloplast outer membrane and peptidoglycan should contain charged phosphate and amino groups and the silicon nitride tip should have a negative charge,[29] so increases in ionic strength would be expected to diminish electrostatic cell−tip interactions. Furthermore, charge screening by additional ions can lead to the contraction of cellular and extracellular polymers.[27,48,49] The tip would be expected to penetrate these compacted layers less readily. Consistent with this hypothesis, we observe a diminished region of nonlinearity in the extension curves of cells exposed to higher ionic strengths (data not shown).

Future Work. Having here established the groundwork for probing bdelloplasts in aqueous buffer by atomic force microscopy, we are currently working to extend our studies to the entire *Bdellovibrio bacteriovorus* 109J life cycle. Directly monitoring the physical changes that occur in individual bdelloplasts over the course of hours will allow us to elucidate how the properties of the invaded cell change during the course of digestion. Measuring the elastic properties of the bdellovibrio predator itself will help to disentangle the contributions of the predator from that of the prey's cytoplasm to the measured elasticity of the bdelloplast. Examining the elasticity and adhesive properties of bdelloplasts derived from other gram-negative prey cells will allow us to explore the role of both predator and prey on bdelloplast structure. Each of these goals presents significant technical challenges that we are currently tackling.

(57) Vadillo-Rodríguez, V.; Busscher, H. J.; Norde, W.; de Vries, J.; van der Mei, H. C. *Microbiology* **2004**, *150*, 1015–1022.

(58) Touhami, A.; Jericho, M. H.; Boyd, J. M.; Beveridge, T. J. *J. Bacteriol.* **2006**, *188*, 370–377.

Conclusions

In this work, we explored the predation on simple bacterial biofilms by the nanoscale predator *Bdellovibrio bacteriovorus* 109J. Biofilm eradication is both challenging and critically important in industrial, medical, and agricultural settings, and the role that bacterial predators such as *Bdellovibrio bacteriovorus* might play in the eradication of biofilms is a promising area of research. AFM images and force curves, obtained in aqueous buffer on the native biofilm during predator attack, illustrated that the *E. coli* prey cells become rounder, shorter, softer, and more adhesive after attack and invasion by the *Bdellovibrio* predator, consistent with biochemical investigations of prey cell modification and degradation by the predator. This work opens up the exciting possibility of imaging and measuring other dynamic events in living unfixed cells.

Acknowledgment. We thank the following people and organizations for their support: Professor J. J. Quinn for her drawing of the *Bdellovibrio* life cycle; Sophia Hohlbauch and Asylum Research for their assistance in establishing critical instrumental and experimental parameters for this work; the NSF RUI program (no. CHE0517998 to M.E.N. and E.M.S); the Clare Boothe Luce foundation (K.E.A. and M.E.N); the Camille and Henry Dreyfus Foundation (E.M.S); HHMI through Occidental College (M.A.F.); the Undergraduate Research Center at Occidental College; the Fund the Future program at Mount Holyoke College (M.E.N.).

Note Added after ASAP Publication. This article was published ASAP on June 24, 2008. Due to a production error, the author's corrections were not included. The correct version was published on July 1, 2008.

Supporting Information Available: Cell spring constant as a function of ionic strength. Tip−cell adhesion for bdelloplasts and *E. coli* cells in HM with 75 and 150 mM NaCl, respectively. Tabulated averages, standard errors, and confidence intervals for all measurements. This material is available free of charge via the Internet at http://pubs.acs.org.

LA8009354